Rhodopsin-Mediated Photoreception in Cryptophyte Flagellates

Oleg A. Sineshchekov,*† Elena G. Govorunova,*†‡ Kwang-Hwan Jung,* Stefan Zauner,‡ Uwe-G. Maier,‡ and John L. Spudich*

*Center for Membrane Biology, Department of Biochemistry and Molecular Biology, University of Texas Medical School, Houston, Texas; †Biology Department, Moscow State University, Moscow, Russia; and ‡Cell Biology, Philipps-University Marburg, Marburg, Germany

ABSTRACT We show that phototaxis in cryptophytes is likely mediated by a two-rhodopsin-based photosensory mechanism similar to that recently demonstrated in the green alga *Chlamydomonas reinhardtii*, and for the first time, to our knowledge, report spectroscopic and charge movement properties of cryptophyte algal rhodopsins. The marine cryptophyte *Guillardia theta* exhibits positive phototaxis with maximum sensitivity at 450 nm and a secondary band above 500 nm. Variability of the relative sensitivities at these wavelengths and light-dependent inhibition of phototaxis in both bands by hydroxylamine suggest the involvement of two rhodopsin photoreceptors. In the related freshwater cryptophyte *Cryptomonas* sp. two photoreceptor currents similar to those mediated by the two sensory rhodopsins in green algae were recorded. Two cDNA sequences from *G. theta* and one from *Cryptomonas* encoding proteins homologous to type 1 opsins were identified. The photochemical reaction cycle of one *Escherichia-coli*-expressed rhodopsin from *G. theta* (*Gt*R1) involves K-, M-, and O-like intermediates with relatively slow (~80 ms) turnover time. *Gt*R1 shows lack of light-driven proton pumping activity in *E. coli* cells, although carboxylated residues are at the positions of the Schiff base proton acceptor and donor as in proton pumping rhodopsins. The absorption spectrum, corresponding to the long-wavelength band of phototaxis sensitivity, makes this pigment a candidate for one of the *G. theta* sensory rhodopsins. A second rhodopsin from *G. theta* (*Gt*R2) and the one from *Cryptomonas* have noncarboxylated residues at the donor position as in known sensory rhodopsins.

INTRODUCTION

Most unicellular flagellate algae are phototactic, i.e., capable of orientation with respect to the direction of light (for review, see Witman (1), Kreimer (2), and Hegemann (3)). Light tracking is based on a periodic shading and irradiation of the photoreceptor during helical swimming (for review, see Foster and Smyth (4)). In addition, an abrupt change in the intensity of ambient light causes a photophobic response—a transient stop or reorientation of the cell movement. Mechanisms of photobehavior have been most studied in *Chlamydomonas reinhardtii* and related chlorophytes, and in the euglenophyte *Euglena gracilis*. Phototaxis and the photophobic response in *Chlamydomonas* are mediated by two sensory rhodopsins, *Chlamydomonas* sensory rhodopsin A (*C*SRA) and B (*C*SRB), photoexcitation of which triggers a cascade of transmembrane electrical currents leading to flagellar motor responses (for recent reviews, see Kateriya et al. (5) and Sineshchekov and Spudich (6)). In contrast, photobehavior in *Euglena* involves a receptor flavoprotein, photoactivated adenylyl cyclase (7,8).

Over the past five years, genomic studies have revealed a broad distribution of rhodopsins in microorganisms in all three domains of life: Archaea, Eubacteria, and Eukarya (9). Many of the rhodopsins are of unknown function; however, within each domain examples of both transporters and sensory receptors have been demonstrated (9–11). *C*SRA and *C*SRB of *Chlamydomonas* are the only known sensory retinylidene receptors in eukaryotic microorganisms for which the function has been proven experimentally (12). The similar photobehavior and photoelectric responses in *Chlamydomonas* and other tested green algae (*Haematococcus, Polytomella, Spermatozopsis, Hafniomonas*, and *Volvox*) indicate that light perception likely involves two rhodopsin photoreceptors in the entire group of chlorophycean flagellates (6). Much less is known about the phototaxis receptors in other systematic groups of flagellates.

Cryptophytes originated from a eukaryotic host cell and a eukaryotic endosymbiont by secondary endosymbiosis (13). Unlike any other flagellate algae, they contain phycobilins as accessory photosynthetic pigments, as do red algae and cyanobacteria. Many cryptophytes demonstrate photobehavior similar to that in *Chlamydomonas* and *Euglena* (reviewed in Watanabe and Erata (14)), but the chemical nature of their phototaxis receptors and the transduction mechanisms have been so far unclear. An early action spectroscopy study in *Cryptomonas* sp. CR-1 suggested phycoerythrin as the phototaxis receptor (15). However, subsequent comparative analysis of phototaxis action spectra in several cryptomonad species containing different phicobilins ruled out this possibility (16).

Submitted July 18, 2005, and accepted for publication August 18, 2005.

Address reprint requests to Oleg A. Sineshchekov, Chair of Physico-Chemical Biology, Biology Department, Moscow State University, Vorobievy Gory, 119992 Moscow, Russia. Tel.: 7-095-9394374; Fax: 7-095-9394309; E-mail: oleg_sinesh@yahoo.com; or to John L. Spudich, Center for Membrane Biology, Dept. of Biochemistry and Molecular Biology, University of Texas Medical School, Houston, TX 77030. Tel.: 713-500-5473; Fax: 713-500-0545; E-mail: John.L.Spudich@uth.tmc.edu.

Kwang-Hwan Jung's present address is Dept. of Life Science and Interdisciplinary Program of Integrated Biotechnology, Sogang University, Seoul 121-742, Korea.

0006-3495/05/12/4310/10 $2.00

doi: 10.1529/biophysj.105.070920

Guillardia theta is a marine cryptophyte used as a model to study plastid evolution. Genomes of both the chloroplast and nucleomorph (a remnant nucleus of the engulfed eukaryotic endosymbiont) of *G. theta* have been completely sequenced (17,18), and generation of a nuclear expressed sequence tags (EST) database is currently under way. A BLAST search of this database revealed a cDNA sequence encoding a protein homologous to microbial (type 1) opsins (9,19).

Here we report analysis of photobehavior in *G. theta* and photoelectric currents in a close relative of *G. theta*—a freshwater *Cryptomonas* species. The results show that photomotility in cryptophytes likely involves a dual rhodopsin-based photosensory system similar to that in chlorophytes. Optical and electrical characteristics of the first known *G. theta* rhodopsin expressed in *Escherichia coli* suggest its possible role as one of the phototaxis receptors. We also report identification of a second rhodopsin species in *G. theta*, and a highly homologous sequence in the phototactic freshwater *Cryptomonas* with characteristics typical of light sensors.

MATERIALS AND METHODS

Strains and culture conditions

G. theta and *Cryptomonas* sp. strain S2 were obtained from the culture collection of algae at Philipps-University Marburg (Marburg, Germany) and grown in liquid salt water medium (20) at 21°C, or in liquid Moor-Chu medium (21) at 15°C, respectively, at a light/dark cycle of 14/10 h (1.28 W m^{-2}) from cool fluorescence lamps. Cultivation of *C. reinhardtii* (strain 495) used for control measurements of photoaccumulation was as described (22). *E. coli* strains DH5α and MRF′ were used for cloning, and strain UT5600 for expression of *G. theta* opsin. *E. coli* transformants were grown in LB (Luria-Bertani) medium in the presence of ampicillin (50 μg/ml) at 37°C.

G. theta EST library construction and analysis

A *G. theta* EST library was constructed by Vertis Biotechnologie (Freising, Germany) and cDNA clones were sequenced from their 5′ ends by MWG-Biotech (Ebersberg, Germany). BLASTX search of GenBank revealed that the clone sg05_004_f10 encodes a protein homologous to type 1 opsins.

Cloning of opsin homologs from *Cryptomonas* sp. S2

Total RNA was extracted from 100 ml of 2-week-old culture of *Cryptomonas* S2 using Trizol reagent (Invitrogen, Karlsruhe, Germany). Synthesis of 3′ and 5′ rapid amplification of cDNA ends (RACE) ready first-strand cDNAs and 3′ and 5′ RACE polymerase chain reaction (PCR) were carried out using SMART RACE cDNA amplification kit (BD Biosciences Clontech, San Jose, CA). 3′ RACE was performed using the forward degenerate primer TAYRYXGAXTGGXTXXTXACXACXCC based on the consensus amino acid residue sequence in the most conserved region of helix C derived from alignment of type 1 opsins. The PCR product was gel-purified, cloned into pGEM-T vector (Promega, Madison, WI), and sequenced. 5′ RACE was performed using the specific reverse primer GATGGTCAACCATGCCACCTTGCC designed according to the sequence of the cloned PCR product ~240 bp downstream from the annealing site of the degenerate primer. Analysis of the PCR product was performed as before. Similar RACE procedures using specific primers were carried out to verify the sequence of *G. theta* opsin from EST272.

Genomic PCR

Genomic PCR was used to test for the presence of introns in the coding regions of the genomic copies of the two *G. theta* opsin sequences. Genomic DNA was isolated from 1-week-old *G. theta* culture using Trizol reagent (Invitrogen, Karlsruhe, Germany). Genomic PCR was performed using *Taq* DNA polymerase (Fermentas, St. Leon-Rot, Germany) and primers based on the coding regions of *G. theta* opsin cDNA sequences. The PCR products were gel-purified, cloned into pGEM-T vector (Promega, Madison, WI), and sequenced.

Construction of an expression plasmid encoding *G. theta* rhodopsin 1

A C-terminal His_6 tag and *Nde*I/*Hind*III restriction sites were introduced by PCR into the fragment of *G. theta* cDNA homologous to type 1 opsins found in EST272 of *G. theta* cloned in a pBluescriptII KS+. The *Nde*I/*Hind*III restriction fragments were subcloned into a modified version of the *E. coli* vector pET-15b (23). From this vector, the constructs were transferred to the *Xba*I/*Hind*III site of a modified *E. coli* expression vector pMS107 (24). The resultant plasmids were partially sequenced to verify correct insertion of the constructs.

Protein expression, purification, and Western blot analysis

E. coli cells transformed with *Guillardia* opsin were grown to $A_{550} = 0.4$ and induced with 1 mM isopropyl-β-D-thiogalactopyranoside and 10 μM all-*trans* retinal. After 4 h, cells were harvested by centrifugation and sonicated in buffer containing 150 mM NaCl and 30 mM Tris-HCl, pH 7.0. Unbroken cells and cell debris were removed by centrifugation for 15 min at 2600 $\times$ *g*. Cell lysates were incubated for 20 min with 1% *n*-dodecyl-β-D-maltopyranoside (Anatrace, Maumee, OH) at 4°C. Nonsolubilized material was removed by a second centrifugation at 20,000 $\times$ *g* for 15 min at 4°C. The supernatant was combined with Ni-NTA agarose (Quiagen, Valencia, CA) and incubated for 4 h on a rotator at 4°C in the presence of 5 mM imidazole. The mixture was washed twice with two bed volumes of 20 mM imidazole and eluted with 250 mM imidazole in the same buffer containing 0.01% *n*-dodecyl-β-D-maltopyranoside. The fractions with the highest A_{280} were collected and dialyzed against the same buffer without imidazole. Protein concentration was measured with the protein assay kit from Bio-Rad Laboratories (Hercules, CA). Proteins in the collected fractions were separated by 12% SDS-PAGE and analyzed with an anti-His_6 antibody (BD Biosciences Clontech) using a standard Western blot protocol.

Spectroscopy

Flash-induced absorption changes were acquired with a laboratory-constructed cross-beam flash-photolysis system. The actinic flash was from an Nd-YAG pulse laser (Continuum, Surelite I, Santa Clara, CA; 532 nm, 6 ns, 40 mJ). Signals from the photomultiplier were amplified by a low-noise current amplifier Keithley 428 (Keithley Instruments, Cleveland, OH), digitized by a DIGIDATA 1320A at 2 μs/point and stored in a PC using the Clampex 9.0 program (both from Axon Instruments, Foster City, CA). We averaged 20–100 transients obtained with a 5-s flash interval. To minimize excitation artifacts, equal numbers of individual sweeps with the measuring beam blocked (scattered light) were averaged and subtracted from the measuring beam-monitored signals.

Photoelectric measurements

Photoinduced electrical signals were recorded in the freshwater cryptophyte *Cryptomonas* sp. S2 by the suspension method described earlier (22).

Asymmetric photocurrents in cells oriented by gravitaxis were picked up by two platinum electrodes placed in the vertical plane. A photoflash (<1 ms duration) in combination with heat-protecting and interference or broadband filters in the blue-green region was used for excitation. Signals were amplified by a model 564 current amplifier (Ithaco, Ithaca, NY). Intramolecular charge movements in *G. theta* opsin were measured in suspensions of *E. coli* cells expressing this pigment. A recently developed approach based on the light-focusing effect within the cells under unilateral 532-nm laser or photoflash excitation was used (25). Data acquisition was as described for spectroscopic measurements (see above).

Measurement of photoaccumulation

Experiments were carried out in *G. theta* cultures between 2 and 3 weeks after inoculation. Photoaccumulation of cells was measured at the illuminated side of a rectangular cuvette (30 × 20 × 1 mm inner dimensions) placed under the microscope. A fresh sample of cells in the growth medium was used for each recording to avoid adaptation. The actinic light was provided by a halogen lamp supplemented with heat-protecting and interference filters (half-bandwidth, 7 nm) (Schott, Mainz, Germany). The monitoring light from a microscope illuminator supplemented with a cutoff filter (>730 nm) was directed at 90° to the actinic light. The optical signal was recorded with a photodiode (FD24K, Kontest, Moscow, Russia) in series with a low-noise current preamplifier (model 564, Ithaco) and digitized by a MiniDigi interface controlled with the Axoscope software (both from Axon Instruments). The Clampfit 9.0 program (Axon Instruments) and Origin 7.0 program (OriginLab Corp., Northhampton, MA) was used for data analysis.

The influence of hydroxylamine on *G. theta* phototaxis was tested under conditions earlier shown to inhibit rhodopsin-mediated phototaxis in chlorophyte flagellates (26). Hydroxylamine or control buffer were added to two identical samples of culture. Pairs of test and control samples were incubated either in the darkness or under continuous illumination with white light (10 W m-2). Fresh aliquots of cells were dispensed from the culture samples for each measurement of photoaccumulation and discarded after use.

RESULTS AND DISCUSSION

G. theta photobehavior

To the best of our knowledge, no photomotility responses have been so far reported in *G. theta*. We measured the net behavioral response of a *G. theta* population to unilateral illumination. Switching on the light induced accumulation of the cells at the illuminated side of the cuvette (positive phototaxis) with a delay of ~5 s (Fig. 1 *A*, *solid traces*). The time course of accumulation was very close to that measured in dark-adapted *C. reinhardtii* (Fig. 1 *A*, *dashed trace*), but the sensitivity of *G. theta* was ~50 times less. Prolonged illumination of a *G. theta* cell sample caused a partial decrease in cell concentration at the illuminated side of the cuvette (not shown) that reflected a drop in the sensitivity of positive phototaxis, or a switch from positive to negative phototaxis due to adaptation.

Switching off the high-intensity light after prolonged illumination resulted in a transient peak of accumulation followed by a slow relaxation of the signal, similar to that in *C. reinhardtii* (Fig. 1 *A*, *upper curves*). It was shown earlier that in an overall positively reacting population of green algae a fraction of cells demonstrates negative phototaxis. Tracking of individual cells for extended periods of time revealed that the direction of oriented swimming alternates periodically between toward and away from the light source (27). In *Chlamydomonas* both positively and negatively reacting cells move predominantly with their photoreceptors orienting outside the helical trajectory (28). This means that the photoreceptor is shaded by the cell body in positively phototactic cells and illuminated in negatively phototactic ones. Taking this into account, a transient acceleration of cell accumulation upon switching off the light can be explained by the preferential temporal reorientation of the cells moving away from the light source. Thus, the kinetics of cell accumulation indicates the existence of negative phototaxis and the step-down photophobic response in *G. theta* in addition to net positive phototaxis. Both positive and negative phototaxis were observed earlier in the marine species *Cryptomonas maculata* (29), whereas the freshwater *Cryptomonas* sp. CR-1 demonstrated exclusively positive phototaxis (15). Step-up, but not step-down, photophobic responses were found in the latter species only at very high light intensities (30).

The area under the accumulation curve over a defined time was used for quantitative analysis of phototaxis. The response magnitude depended logarithmically on the light intensity. The spectral sensitivity of net positive phototaxis was determined as the reciprocal of light intensities which resulted in an equal response (e.g., by the shift of a light-intensity curve for each wavelength as compared to the response at the reference wavelength of 500 nm). The spectral dependence of photoaccumulation has the main maximum at 450 nm with a clear shoulder above 500 nm (Fig. 1 *B*, *columns*). The shape of the spectral dependence with an unusually large half-bandwidth indicates the involvement of more than one pigment in photoreception. This conclusion is further corroborated by a change in relative spectral efficiency of 450 nm and 500 nm light observed upon prolonged illumination (Fig. 1 *C*).

A possible explanation for the similarly broad action spectra of photoelectric and motility responses measured earlier in the green alga *Haematococcus pluvialis* is the organization of the phototaxis receptors similar to photosynthetic units, which entail energy transfer from an antenna to a reaction center (31). The complex pronounced fine structure of these spectra (not characteristic for rhodopsins) suggested that energy could migrate from carotenoids or flavins. However, the very high light saturation of the electrical responses excluded the existence of a large and efficient light-harvesting antenna in this organism (32). Later it was demonstrated that two rhodopsins of the related chlorophyte *C. reinhardtii* function independently in different spectral bands (12). This favors the involvement of two independent rhodopsin receptors also in phototaxis of *G. theta*, although energy migration within each receptor system cannot be excluded.

Hydroxylamine causes a light-dependent cleavage of retinylidene chromophores from rhodopsins and inhibits phototaxis in the chlorophytes *C. reinhardtii* (33) and

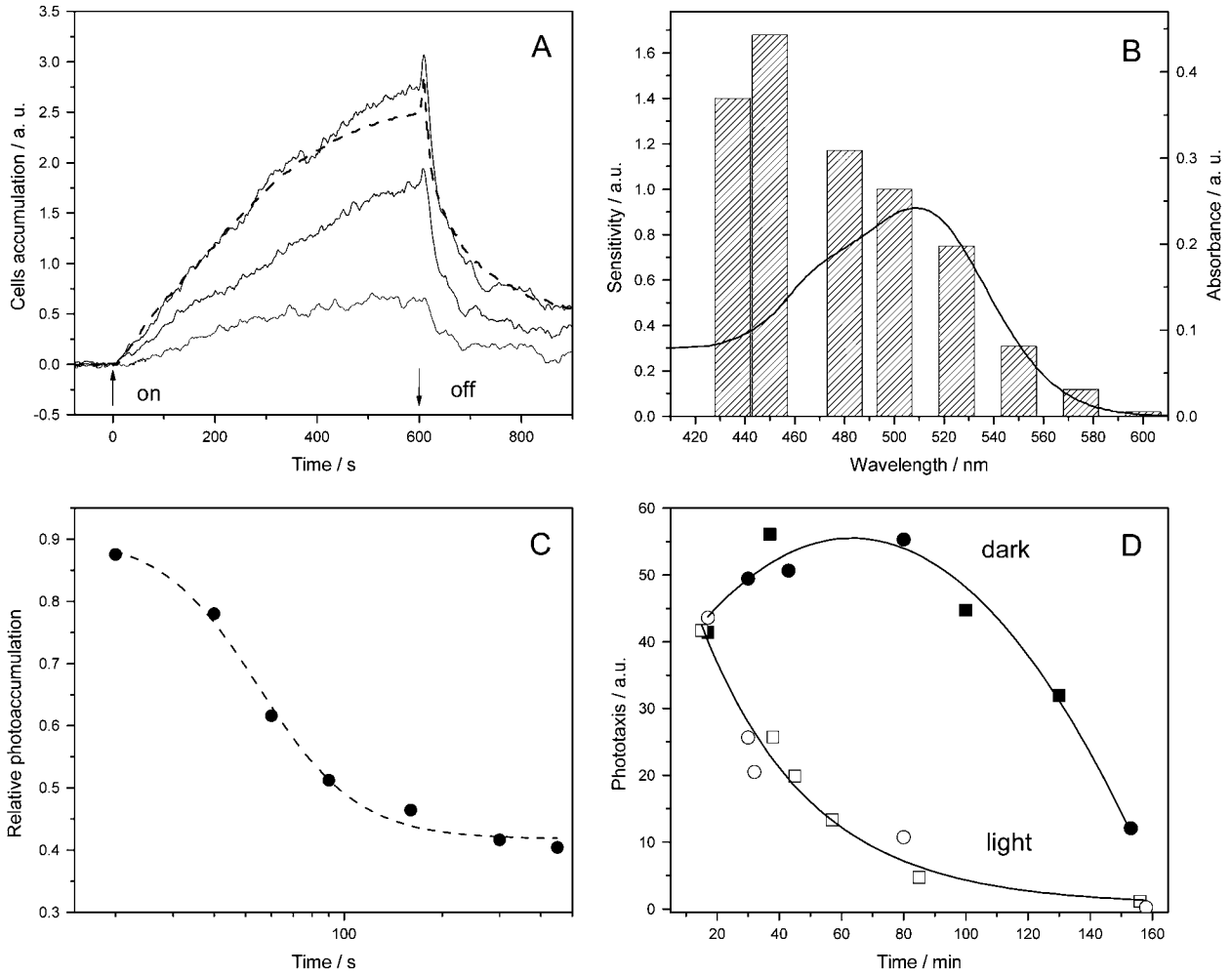

FIGURE 1 (*A*) The time course of photoaccumulation of *G. theta* cells (*solid lines*) and control *C. reinhardtii* cells (*dashed line*) at the illuminated side of the cuvette in response to 500 nm actinic light. The arrows indicate switching on and off the actinic light. The relative light intensities were, from top to bottom, 100%, 26.5%, and 7.5% for *G. theta*, and 2% for *C. reinhardtii*. (*B*) Spectral sensitivity of *G. theta* phototaxis. Bars represent the reciprocal of equal response quantum requirement for photoaccumulation during 50 s, calculated on the basis of fluence-response curves; the solid line represents the absorption spectrum of purified *Gt*R1. (*C*) Decrease in the relative sensitivity to long-wavelength light during actinic light stimulation. The ratio of the amplitudes of photoaccumulation by 500 nm and 450 nm is plotted as a function of the duration of actinic illumination. (*D*) Light-dependent inhibition of phototaxis in *G. theta* by hydroxylamine (1 mM final concentration). The photoaccumulation during 100 s after the onset of the actinic light is plotted as a function of incubation time of the sample in darkness (*solid symbols*) or under 10 W m^{-2} white light (*open symbols*). Squares, 450 nm actinic light; circles, 500 nm actinic light.

H. pluvialis (26). In *C. reinhardtii* rhodopsin receptors for phototaxis have been identified at the molecular level (12), whereas in *H. pluvialis* the presence of similar receptors was deduced from analysis of photoinduced electric currents (6). Illumination of *G. theta* culture in the presence of 1 mM hydroxylamine induced progressive inhibition of phototaxis to both short- and long-wavelength light, as compared to the dark conditions (Fig. 1 *D*). Therefore, it is likely that photoreception at both 450 and 510 nm is mediated by rhodopsin pigments.

As we show below, the maximal absorption of the first known *G. theta* rhodopsin functionally expressed in *E. coli* cells (Fig. 1 *B*, *solid line*, and see Fig. 5 *A*) corresponds to the long-wavelength shoulder of the spectral sensitivity of phototaxis. This result points to the possible role of this protein as one of the phototaxis receptors.

Photoinduced electrical signals in a freshwater cryptophyte

Measurement of photoinduced electrical currents in suspensions of marine flagellates, such as *G. theta*, is not technically possible due to the high ionic strength of seawater. Instead, we used a related cryptophyte, the freshwater *Cryptomonas* sp. S2. Phototactic orientation in this species has been reported earlier (34). Only small photocurrents were recorded under unilateral excitation from nonoriented suspensions of this alga, which was expected, taking into account its lack of an

eyespot and, consequently, inefficient shading. Similar to green flagellates, cryptophytes demonstrate pronounced gravitaxis (35). Therefore, electrical measurements were carried out in the gravipreoriented mode, which provides a higher sensitivity of measurements, as compared to measurements in nonoriented cell suspensions, and allows determination of the localization of light-induced currents (22).

A light flash induces a photoelectric signal, which comprises two kinetically resolved currents in the time domain characteristic for photoreceptor currents in green flagellates (Fig. 2 *A*). Two components can be distinguished in both the rise and decay of the signal in *Cryptomonas*, as in green flagellates (36). At least one of the currents in *Cryptomonas* has a light-dependent delay (Fig. 2 *B*), as is characteristic of the delayed photoreceptor current in *Chlamydomonas* and related green algae (37). The fluence-response dependence of the peak amplitude of the photocurrent in *Cryptomonas* reveals low- and high-saturating components (Fig. 2 *B*, *inset*), which is again typical of photoreceptor currents in green flagellates (37) and reflects contributions of the two receptor rhodopsins (12). Thus, the features of the two currents in *Cryptomonas* strongly indicate that they are photoreceptor currents of phototaxis. This indication is further corroborated by their spectral sensitivity and dependence on the extracellular concentration of Ca^{2+} ions (not shown).

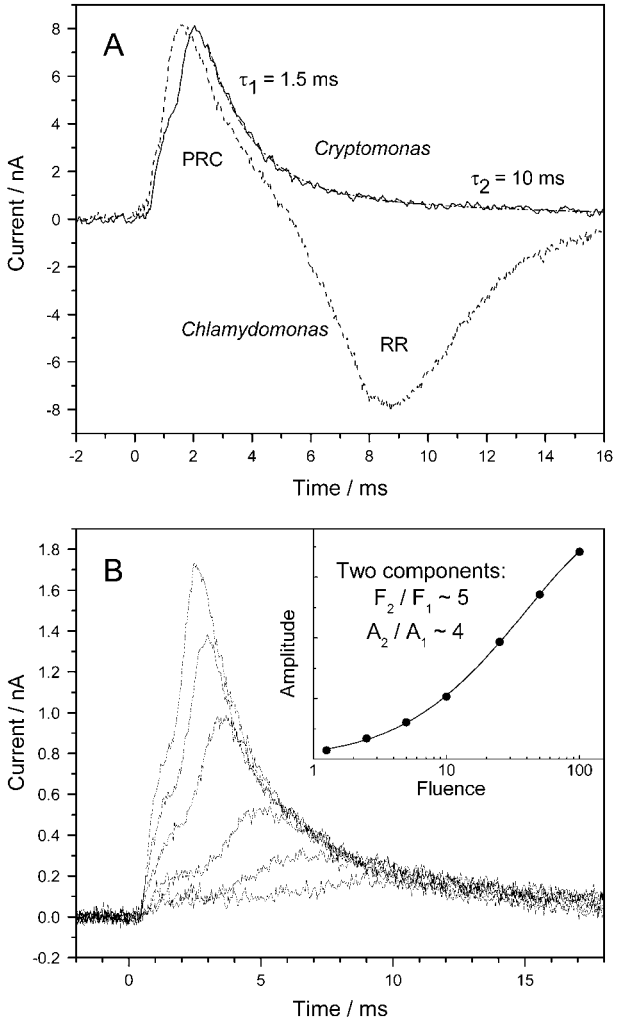

FIGURE 2 Photoinduced electrical signals in *Cryptomonas sp*. S2: a freshwater relative of *G. theta*. (*A*) Kinetics of light-induced currents (*solid line*) and a two-exponential fit of the current decay (*dash-dotted line*). The sign of the photoelectric signal measured under the same conditions in the flagellate green alga *C. reinhardtii* (*dashed line*) was inverted for easier comparison with the signal in *Cryptomonas*. PRC, photoreceptor current; RR, regenerative response. (*B*) A series of photoelectric signals in *Cryptomonas* measured at different flash intensities. (*Inset*) Fluence dependence of the photoreceptor current and its fitting with a two-exponential function (*solid line*). F_2/F_1 and A_2/A_1 are the ratios of computer-generated estimates for saturation levels and maximal amplitudes, respectively, of the first and second components.

The two photoreceptor currents in *Cryptomonas* are slower and the difference between their kinetic parameters is larger compared to those of *Chlamydomonas* and other green flagellates. On the other hand, the ratio between the saturation levels of the low- and high-saturation currents is smaller than that observed in green flagellates (Fig. 2 *B*, *inset*). No regenerative electrical response could be detected in *Cryptomonas* (Fig. 2 *A*, *solid trace*), which was expected taking into account a very high threshold for the step-up photophobic response known in this genus (30).

The sign of photoelectrical signals recorded from cell suspensions in preoriented mode reflects localization of the current generators within the cell. The sign of photoreceptor currents in *Cryptomonas* is opposite to that in *C. reinhardtii*, which means that the photoreceptive structure is localized in *Cryptomonas* closer to the anterior flagella-bearing end of the cell. A similar situation has been described earlier in the green flagellate *H. pluvialis* (22).

Summarizing the results of behavioral and electrical measurements, we conclude that photobehavior in cryptophytes likely involves the same basic scheme of photoreception and transduction as recently found in *Chlamydomonas* (12) and suggested for other green flagellates (6). Namely, two rhodopsins that absorb in different spectral bands and optimally function at different intensity ranges generate two photoreceptor currents that control flagella movement during phototaxis. Below we describe molecular candidates for these receptor pigments.

Primary sequences of cryptophyte opsins

The first *G. theta* cDNA sequence encoding protein homologous to type 1 opsins has been identified earlier in EST272 (GenBank accession number AW342219). More careful analysis of the original plasmid revealed an extra basepair in the coding region, which has been confirmed by RACE PCR using total RNA isolated from *G. theta*. A corrected sequence has been submitted to GenBank (accession number DQ133529). We designated the encoded protein, when complexed with retinal, as *Gt*R1 (*G. theta*

rhodopsin 1). The protein encoded by *G. theta* cDNA from EST clone sg05_004_f10 (accession number DQ133530), when complexed with retinal, was named *Gt*R2 (*G. theta* rhodopsin 2). The homologous protein encoded by the cDNA sequence identified by degenerate RACE PCR in the freshwater *Cryptomonas* sp. S2 (accession number DQ133531), when complexed with retinal, was designated as *C*R (*Cryptomonas* rhodopsin).

None of the three encoded proteins extends more than 20 residues after the predicted end of helix G of their seven-transmembrane (7TM) domains, in contrast to *Chlamydomonas* sensory rhodopsins, which have bulky C-terminal domains consisting of ~400 amino acid residues. Photobehavioral and photoelectric responses in cryptophyte flagellates are very similar to those in *Chlamydomonas* (Figs. 1 and 2). If the rhodopsins reported here in cryptophytes mediate these responses, it would follow that the presence of a large C-terminal domain attached to the 7TM rhodopsin domain as in *C*SRA and *C*SRB is not critical for response generation. It is possible that these domains do indeed play a critical role in signaling but that they exist in cryptophytes on other proteins separate from the 7TM domains. On the other hand, the phototactic sensitivity of *G. theta* is ~50-fold less than that of *C. reinhardtii*, which would be consistent with the C-terminal domains of *Chlamydomonas* rhodopsins functioning in signal amplification. Alternatively, these domains may play a regulatory role. Such auxiliary roles of the C-terminal domains are supported by the observation that the full-length sequences and 7TM domains of *Chlamydomonas* rhodopsins both exhibit identical ion channel activities when heterologously expressed in *Xenopus* oocytes (38,39). It has not yet been proven, however, that the channel activity observed in oocytes triggers the photosensory cascade in host *Chlamydomonas* cells. Therefore, the involvement of the C-domains in signal generation cannot be excluded.

The presence of polyA tails in all three cDNA sequences and the presence of introns in genomic copies of sequences encoding for *Gt*R1 and *Gt*R2, as revealed by genomic PCR, confirm their eukaryotic origin. Although we have so far identified only one opsin cDNA sequence in freshwater *Cryptomonas*, the characteristics of photoreceptor currents in this microorganism strongly suggest the existence of a second opsin species. However, low homology between even the most conserved regions in the primary sequences of type 1 opsins hinder their identification by degenerate PCR, and no EST or other genomic data are at present available for freshwater *Cryptomonas*.

ClustalW alignment of cryptophyte and other microbial opsins in the region corresponding to helix C is shown in Fig. 3. Amino acid residues that form the retinal-binding pocket in bacteriorhodopsin (BR) and *Natronomonas pharaonis* sensory rhodopsin II, as revealed by x-ray crystallography (40,41), are highly conserved in all three cryptophyte opsins, including the Schiff base proton acceptor (Asp^{85} in BR). A noncarboxylated residue in the place of the Schiff base

FIGURE 3 Alignment of helix C regions of primary sequences of opsins from cryptophyte algae (protein names in boldface) and other type 1 opsins. Amino acid residues forming the retinal-binding pocket are marked with an asterisk. Carboxylated amino acid residues corresponding to the proton acceptor (Asp^{85}) and proton donor (Asp^{96}) in *Hs*BR are shaded black. *Hs*BR, *Halobacterium salinarum* bacteriorhodopsin; GPR, green-absorbing proteorhodopsin; BPR, blue-absorbing proteorhodopsin; *Np*SRII, *Natronomonas pharaonis* sensory rhodopsin II.

proton donor (Asp^{96} in BR) is a hallmark of sensory rhodopsins from Archaea and *Chlamydomonas*, as well as of *Anabaena* sensory rhodopsin (ASR), a sensory function of which has been deduced from its properties (10,42,43). *Gt*R2 and *C*R also have noncarboxylated residues at this position, which argues for their action as light sensors rather than proton pumps. *C*R is unusual in that it contains a His residue (instead of an Arg) corresponding to Arg^{82} of BR, a nearly universally conserved residue in type 1 rhodopsins (9,44). In contrast to *Gt*R2 and *C*R, *Gt*R1 contains Glu in the place of the proton donor, as do proteorhodopsins. We expressed the respective cDNA sequence in *E. coli* and characterized the photochemical and photoelectrical properties of the encoded protein.

Characterization of *Gt*R1 expressed in *E. coli*

The predicted topology of *Gt*R1 reveals seven-transmembrane helices typical of other retinylidene proteins (Fig. 4 *A*). We expressed in *E. coli* two versions of the plasmid,

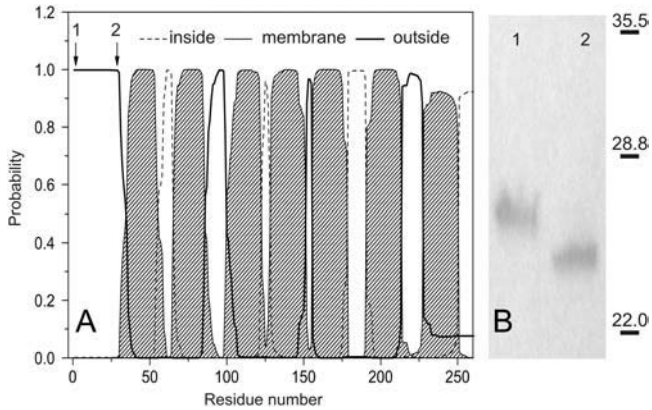

FIGURE 4 (*A*) Transmembrane topology of *Gt*R1 as predicted by TMHMM server version 2.0 (50). Arrows indicate the beginning of the long (*1*) and truncated (*2*) versions of the expressed protein. (*B*) Western blot analysis of long (*1*) and truncated His_6-tagged (*2*) *G. theta* opsins expressed in *E. coli*. Numbers at the right indicate molecular weight markers.

differing in the length of the incorporated *G. theta* cDNA fragment: 1), pGui267, encoding for a polypeptide of 261 amino acid residues (all of the coding region present in the cDNA clone) plus a His_6 tag; 2), pGui239, encoding for a truncated polypeptide, in which 28 amino acid residues predicted to be located outside the membrane were removed from the N-terminus, plus a His_6 tag. The EST sequence contained no start codon, so in both cases it was added artificially. Identification of a complete sequence of the N-terminus of *Gt*R1 is pending. The length of the N-terminus of the truncated sequence corresponds to that of ASR, which is characterized by a high level of functional expression in *E. coli* (10). The site of truncation is schematically shown in Fig. 4 *A*. Western blot analysis of the partially purified proteins indicated approximately the same level of expression of both long and truncated versions in *E. coli* (Fig. 4 *B*).

Both versions of *Gt*R1 expressed in *E. coli* in the presence of all-*trans* retinal form photoactive pigments. The maximum of the absorption spectrum of the purified long pigment is at 509 nm (Fig. 5 *A*), which corresponds to the position of the long-wavelength band of the spectral sensitivity of *G. theta* phototaxis (Fig. 1 *B*). The absorption spectrum of the truncated version of *Gt*R1 is slightly shifted to shorter wavelengths (Fig. 5 *A*).

The main difference between the long and truncated versions of *Gt*R1 is in the rates of their photochemical cycles (Fig. 5 *C*). The photocycle turnover time of the long version of *Gt*R1 in *E. coli* cells is ~85 ms. This is slower than the rates of photocycles in typical ion pumps. For example, under identical conditions, a typical surface-water green-absorbing proteorhodopsin (45) has a turnover time more than an order of magnitude faster than that of *Gt*R1 (46). On

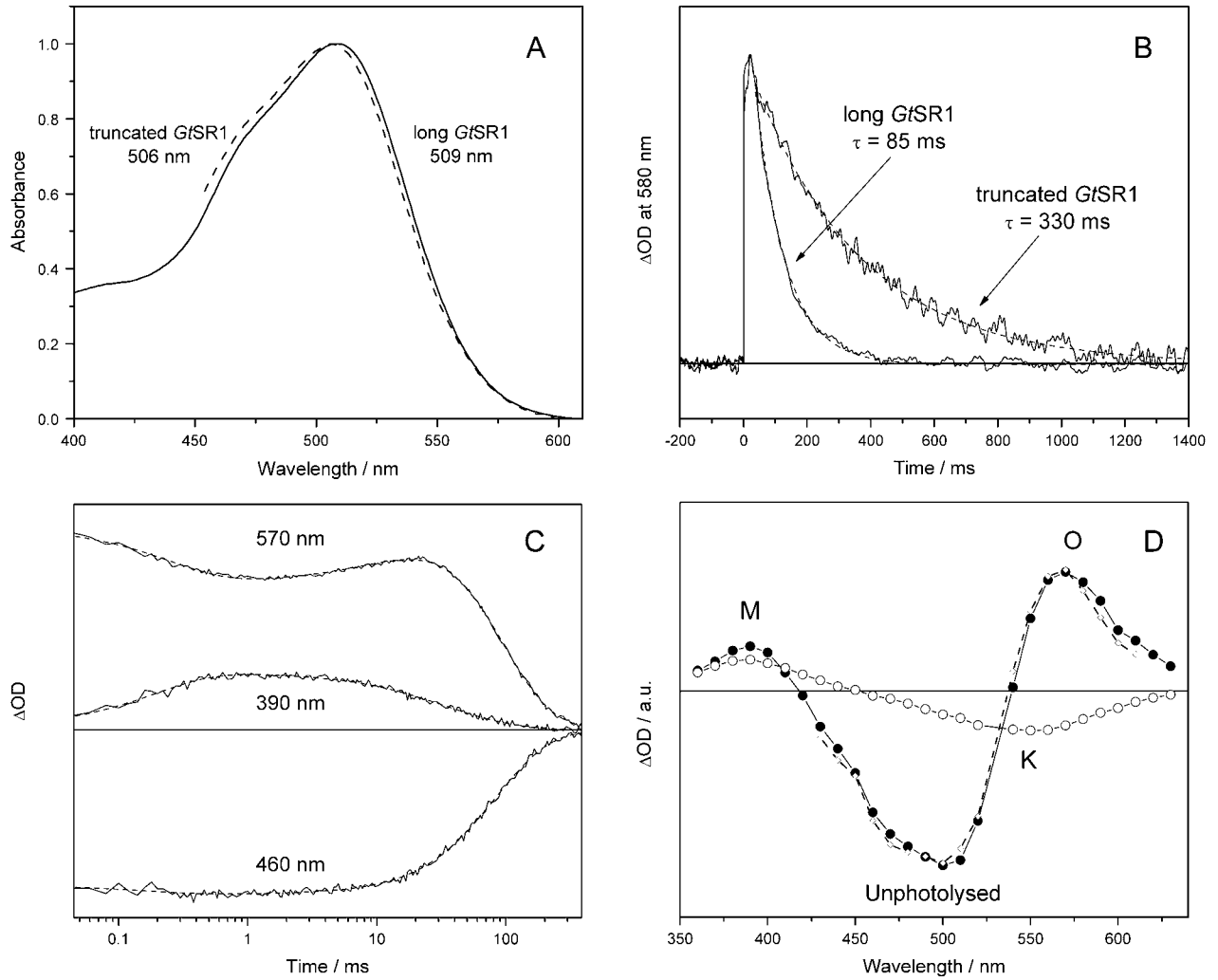

FIGURE 5 (*A*) Absorption specta of purified long (*solid line*) and truncated (*dashed line*) *Gt*R1. (*B*) Laser flash-induced absorbance changes at 580 nm in long and truncated versions of *Gt*R1 expressed in *E. coli* cells (*solid lines*) and fits of their decay with exponential functions (*dashed lines*). (*C*) Kinetics of laser flash-induced absorbance changes in purified long *Gt*R1 at characteristic wavelengths, indicated in the figure, and their multiexponential fitting (*dashed lines*). (*D*) Spectra of laser flash-induced absorbance changes in long *Gt*R1. Solid circles and open circles represent 1 − 0 ms and 1 − 50 μs in purified protein, respectively; open diamonds represent 10 − 0 ms in *Gt*R1 in *E. coli* cells.

the other hand, the rate of the photocycle in *Gt*R1 is comparable to that of the sensory receptor ASR (10,43), and is fast enough for repetitive detection of light in cells rotating at ~2 Hz during swimming. The photocycle of the truncated version of *Gt*R1 is almost fourfold slower than that of the long version (Fig. 5 *B*). We are not aware of other examples of dependence of photochemical characteristics of a rhodopsin on the length of the N-terminus, although a structural influence of the N-terminal segment on the 7TM domain has been reported in animal visual rhodopsin (47). A possible explanation of this effect is that the long N-terminus facilitates proper folding of *Gt*R1. Alternatively, interaction of the N-terminus with the outer half-channel of *Gt*R1 may modify the cycle. Examples of the influence of such ''long-distance'' effects on photochemical properties of the pigments are represented by interactions between ASR and its soluble transducer protein (10,43), or between archaeal sensory rhodopsins and their membrane-bound transducers (48).

The photochemical cycle was investigated in more detail in the purified long version of *Gt*R1, which presumably represents a closer-to-native state of the pigment. Laser flash-induced absorbance changes at characteristic wavelengths are shown in Fig. 5 *C*. The first detected red-shifted K intermediate decays with $\tau \sim 0.2$ ms in parallel with the appearance of a blue-shifted M intermediate. The maxima of the differential absorption spectra corresponding to K and M intermediates are at 550 nm and 390 nm, respectively (Fig. 5 *D*, *open circles*). The M intermediate decays slowly, with two kinetic components, $\tau_1 \sim 25$ ms and $\tau_2 \sim 77$ ms. The rates of these components of the M decay correspond to the rates of the appearance and decay, respectively, of a long-wavelength O intermediate with a maximum at ~570 nm in the differential spectra. This correspondence indicates that M and O intermediates are in equilibrium. The flash-induced differential absorption spectrum of *Gt*R1 measured in intact *E. coli* cells is very similar to that of the purified protein (Fig. 5 *B*, *open diamonds*).

The pumping activity of rhodopsins functionally expressed in *E. coli* is manifested by the outward direction of the overall charge movement upon photostimulation (25). Blue-absorbing proteorhodopsin (BPR), which has the same residues at proton donor and acceptor positions and a turnover time of the cycle very similar to that of *Gt*R1, acts as a typical proton pump (Fig. 6, *upper trace*). In contrast, no significant outward charge transfer has been detected in *E. coli* cells expressing *Gt*R1 (Fig. 6, *lower trace*). In fact, *Gt*R1 shows a small transient positive charge movement in the inward direction. The absence of a pronounced outward positive charge transfer is characteristic of known sensory rhodopsins (e.g., archaeal sensory rhodopsins and ASR (25)). Lack of proton-pumping activity has also been found in heterologously expressed *Neurospora* rhodopsin (49), which has carboxylated residues at both the Schiff base proton donor and acceptor positions, as does *Gt*R1. The lack of *Gt*R1 proton pumping was further confirmed by the absence of light-induced acidification of the external medium in *E. coli* cells expressing this protein (data not shown).

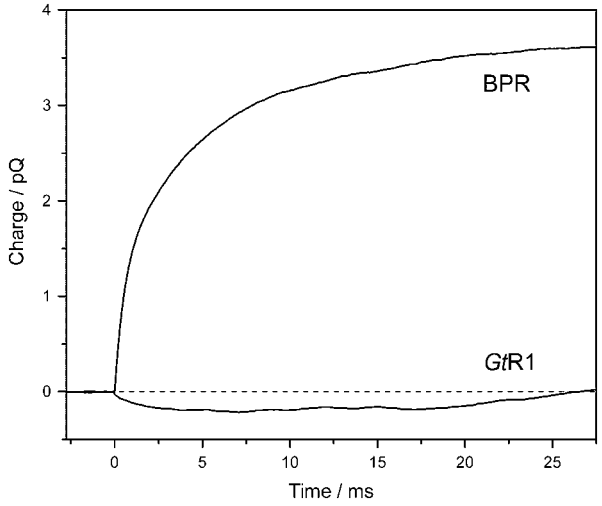

FIGURE 6 Light-induced charge movement in *Gt*R1 and BPR measured in suspension of *E. coli* cells. Positive signal corresponds to transfer of a positive charge to outside the cell.

CONCLUSIONS AND PERSPECTIVES

The cryptophyte *G. theta* exhibits photomotility responses similar to those seen in well-characterized green flagellate algae. Spectral characteristics of these responses, their sensitivity to hydroxylamine bleaching, and photoelectric currents measured in a related freshwater cryptophyte indicate that photobehavior in cryptophyte flagellates likely involves two spectrally different rhodopsin receptors, as occurs in the model green alga *C. reinhardtii*. Two cDNA sequences encoding proteins homologous to type 1 opsins were identified in *G. theta*, and one sequence was identified in the freshwater relative of *G. theta*, *Cryptomonas* sp. S2. Non-carboxylated residues at the acceptor position in *Gt*R2 and *C*R indicate sensory rather than proton pumping functions of these proteins. The photocycling and electrical properties of the *E. coli*-expressed *Gt*R1 are in favor of this rhodopsin also functioning as a light sensor. To test whether these candidates are the photoreceptor pigments of phototaxis by the RNA*i* approach used successfully in *Chlamydomonas* (12), development of transformation techniques for cryptophytes is highly desirable.

To our knowledge, *Gt*R1 is the first algal rhodopsin purified in amounts sufficient for direct flash-photolysis examination of the photochemical cycle and charge motion measurements. The apoproteins of *C*SRA and *C*SRB from *Chlamydomonas* have not formed functional pigments with retinal when expressed in *E. coli* or yeast (12), or other systems suitable for high-scale production of rhodopsins (K. Ridge, University of Texas, Houston, personal communication, 2003). Neither rhodopsin phototaxis receptor has

been isolated directly from its native eukaryotic hosts because of extremely low concentrations of these proteins. Therefore, a possibility, reported here, of obtaining large amounts of an algal, namely, *G. theta* rhodopsin, by overexpression in *E. coli* is especially attractive for future spectroscopic, electrical, and crystallization studies.

We thank the following members of the evolutionary biology group at Philipps-University Marburg, Marburg, Germany: Dr. K. Wenderoth and C. Zimmermann for cultures of cryptophytes and advice on their handling; S. Gould for analysis of *G. theta* EST data; O. Kawach and C. Voβ for DNA sequencing; and M. Sommer, C. Klemme, K. Bolte, K. Jaschinski, J. Büchel, and T. Ammon for help with molecular cloning techniques. We also thank Prof. S. A. Lukyanov (Shemyakin and Ovchinnikov Institute of Bioorganic Chemistry, Moscow, Russia) for advice on using the SMART RACE cDNA amplification kit.

This work was supported by National Science Foundation grant 0091287, National Institutes of Health grant R37GM27750, the Robert A. Welch Foundation, the Russian Foundation for Basic Research grant 05-04-48805, the Deutsche Forschungsgemeinschaft (SFB-TR1), and a follow-up grant from the Alexander von Humboldt Foundation to E.G.G.

REFERENCES

1. Witman, G. B. 1993. *Chlamydomonas* phototaxis. *Trends Cell Biol.* 3:403–408.
2. Kreimer, G. 1994. Cell biology of phototaxis in flagellate algae. *Int. Rev. Cytol.* 148:229–310.
3. Hegemann, P. 1997. Vision in microalgae. *Planta.* 203:265–274.
4. Foster, K.-W., and R. D. Smyth. 1980. Light antennas in phototactic algae. *Microbiol. Rev.* 44:572–630.
5. Kateriya, S., G. Nagel, E. Bamberg, and P. Hegemann. 2004. ''Vision'' in single-celled algae. *News Physiol. Sci.* 19:133–137.
6. Sineshchekov, O. A., and J. L. Spudich. 2005. Sensory rhodopsin signaling in green flagellate algae. *In* Handbook of Photosensory Receptors. W. R. Brigg, and J. L. Spudich, editors. Wiley-VCH, Weinheim, Germany. 25–42.
7. Iseki, N., S. Matsunaga, A. Murakami, K. Ohno, K. Shiga, K. Yoshida, M. Sugai, T. Takahashi, T. Hori, and M. Watanabe. 2002. A blue-light-activated adenylyl cyclase mediates photoavoidance in *Euglena* gracilis. *Nature.* 415:1047–1051.
8. Ntefidou, M., M. Iseki, M. Watanabe, M. Lebert, and D.-P. Häder. 2003. Photoactivated adenylyl cyclase controls phototaxis in the flagellate *Euglena gracilis*. *Plant Physiol.* 133:1517–1521.
9. Jung, K.-H., and J. L. Spudich. 2004. Microbial rhodopsins: transport and sensory proteins throughout the three domains of life. *In* CRC Handbook of Organic Photochemistry and Photobiology. W. H. Horspool and F. Lenci, editors. CRC Press, Boca Raton. 1–12.
10. Jung, K.-H., V. D. Trivedi, and J. L. Spudich. 2003. Demonstration of a sensory rhodopsin in eubacteria. *Mol. Microbiol.* 47:1513–1522.
11. Waschuk, S. A., A. G. Bezerra, Jr., L. Shi, and L. S. Brown. 2005. *Leptosphaeria* rhodopsin: bacteriorhodopsin-like proton pump from a eukaryote. *Proc. Natl. Acad. Sci. USA.* 102:6879–6883.
12. Sineshchekov, O. A., K.-H. Jung, and J. L. Spudich. 2002. Two rhodopsins mediate phototaxis to low- and high-intensity light in *Chlamydomonas reinhardtii*. *Proc. Natl. Acad. Sci. USA.* 99:8689–8694.
13. Stoebe, B., and U.-G. Maier. 2002. One, two, three: nature's tool box for building plastids. *Protoplasma.* 219:123–130.
14. Watanabe, M., and M. Erata. 2001. Yellow-light sensing phototaxis in cryptomonad algae. *In* Comprehensive Series in Photosciences. D.-P. Häder, and M. Lebert, editors. Elsevier, Amsterdam. 343–373.
15. Watanabe, M., and M. Furuya. 1974. Action spectrum of phototaxis in a cryptomonad alga, *Cryptomonas* sp. *Plant Cell Physiol.* 15:413–420.
16. Erata, M., M. Kubota, T. Takahashi, I. Inouye, and M. Watanabe. 1995. Ultrastructure and phototactic action spectra of two genera of cryptophyte flagellate algae, *Cryptomonas* and *Chroomonas*. *Protoplasma.* 188:258–266.
17. Douglas, S. E., and S. L. Penny. 1999. The plastid genome of the cryptophyte alga, *Guillardia theta*: complete sequence and conserved synteny groups confirm its common ancestry with red algae. *J. Mol. Evol.* 48:236–244.
18. Douglas, S., S. Zauner, M. Fraunholz, M. Beaton, S. Penny, L. T. Deng, X. Wu, M. Reith, T. Cavalier-Smith, and U.-G. Maier. 2001. The highly reduced genome of an enslaved algal nucleus. *Nature.* 410:1091–1096.
19. Ruiz-Gonzalez, M. X., and I. Marin. 2004. New insights into the evolutionary history of type 1 rhodopsins. *J. Mol. Evol.* 58:348–358.
20. Guillard, R. R. L. 1975. Culture of phytoplankton for feeding marine invertebrates. *In* Culture of Marine Invertebrate Animals. W. L. Smith, and M. H. Chanley, editors. Plenum Press, New York. 26–60.
21. von Stosch, H. A. 1973. Observations on vegetative reproduction and sexual light cycles of two freshwater dinoflagellates, *Gymnodinium pseudopalustre* Schiller and *Woloszynskia apiculta* sp. nov. *Brit. Phycol. J.* 8:105–134.
22. Sineshchekov, O. A., E. G. Govorunova, A. Der, L. Keszthelyi, and W. Nultsch. 1992. Photoelectric responses in phototactic flagellated algae measured in cell suspension. *J. Photochem. Photobiol. B.* 13:119–134.
23. Jung, K.-H., E. N. Spudich, V. D. Trivedi, and J. L. Spudich. 2001. An archaeal photosignal-transducing module mediates phototaxis in *Escherichia coli*. *J. Bacteriol.* 183:6365–6371.
24. Surette, M. J., and J. B. Stock. 1996. Role of alpha-helical coiled-coil interactions in receptor dimerization, signaling, and adaptation during bacterial chemotaxis. *J. Biol. Chem.* 271:17966–17973.
25. Sineshchekov, O. A., and J. L. Spudich. 2004. Light-induced intramolecular charge movements in microbial rhodopsins in intact *E. coli* cells. *Photochem. Photobiol. Sci.* 3:548–554.
26. Sineshchekov, O. A., E. G. Govorunova, and F. F. Litvin. 1991. The rhodopsin-like photoreceptor in *Haematococcus*: hydroxylamine effect on photoelectric responses and phototaxis of cells. *Sensornye Systemy.* 5:51–55.
27. Sineshchekov, O. A., and E. G. Govorunova. 1991. Rhythmic motion activity of unicellular flagellated algae and its role in phototaxis. *Biofizika.* 36:603–608.
28. Isogai, N., R. Kamiya, and K. Yoshimura. 2000. Dominance between the two flagella during phototactic turning in *Chlamydomonas*. *Zoological Sci.* 17:1261–1266.
29. Häder, D.-P., E. Rhiel, and W. Wehrmeyer. 1987. Phototaxis in the marine flagellate, *Cryptomonas maculata*. *J. Photochem. Photobiol. B.* 1:115–122.
30. Kaneda, H., and M. Furuya. 1986. Temporal changes in swimming direction during the phototactic orientation of individual cells in *Cryptomonas* sp. *Plant Cell Physiol.* 27:265–272.
31. Sineshchekov, O. A., and F. F. Litvin. 1982. Photoregulation of movement in microorganisms. *Uspekhi Mikrobiologii.* 17:62–87.
32. Sineshchekov, O. A. 1991. In Light in Biology and Medicine. Vol. II. R. D. Douglas, editor. Plenum Press, New York. 523–532.
33. Hegemann, P., U. Hegemann, and K.-W. Foster. 1988. Reversible bleaching of *Chlamydomonas reinhardtii* rhodopsin in vivo. *Photochem. Photobiol.* 48:123–128.
34. Rhiel, E., D.-P. Häder, and W. Wehrmeyer. 1988. Photo-orientation in a freshwater *Cryptomonas* species. *J. Photochem. Photobiol. B.* 2:123–132.
35. Rhiel, E., D.-P. Häder, and W. Wehrmeyer. 1988. Diaphototaxis and gravitaxis in a freshwater *Cryptomonas*. *Plant Cell Physiol.* 29:755–760.
36. Sineshchekov, O. A., F. F. Litvin, and L. Keszthelyi. 1990. Two components of photoreceptor potential of the flagellated green alga *Haematococcus pluvialis*. *Biophys. J.* 57:33–39.

37. Sineshchekov, O. A., and E. G. Govorunova. 1999. Rhodopsin-mediated photosensing in green flagellated algae. *Trends Plant Sci.* 4:58–63.

38. Nagel, G., D. Ollig, M. Fuhrmann, S. Kateriya, A. M. Musti, E. Bamberg, and P. Hegemann. 2002. Channelrhodopsin-1: a light-gated proton channel in green algae. *Science*. 296:2395–2398.

39. Nagel, G., T. Szellas, W. Huhn, S. Kateriya, N. Adeishvili, P. Berthold, D. Ollig, P. Hegemann, and E. Bamberg. 2003. Channelrhodopsin-2, a directly light-gated cation-selective membrane channel. *Proc. Natl. Acad. Sci. USA*. 100:13940–13945.

40. Luecke, H., B. Schobert, H. T. Richter, J. P. Cartailler, and J. K. Lanyi. 1999. Structural changes in bacteriorhodopsin during ion transport at 2 Angstrom resolution. *Science*. 286:255–260.

41. Luecke, H., B. Schobert, J. K. Lanyi, E. N. Spudich, and J. L. Spudich. 2001. Crystal structure of sensory rhodopsin II at 2.4 angstroms: insights into color tuning and transducer interaction. *Science*. 293: 1499–1503.

42. Vogeley, L., O. A. Sineshchekov, V. D. Trivedi, J. Sasaki, J. L. Spudich, and H. Luecke. 2004. *Anabaena* sensory rhodopsin: a photochromic color sensor at 2.0 Å. *Science*. 306:1390–1393.

43. Sineshchekov, O. A., V. D. Trivedi, J. Sasaki, and J. L. Spudich. 2005. Photochromicity of *Anabaena* sensory rhodopsin, an atypical microbial receptor with a *cis*-retinal light-adapted form. *J. Biol. Chem.* 280: 14663–14668.

44. Imasheva, E. S., S. P. Balashov, T. G. Ebrey, N. Chen, R. K. Crouch, and D. R. Menick. 1999. Two groups control light-induced Schiff base deprotonation and the proton affinity of Asp^{85} in the Arg^{82}His mutant of bacteriorhodopsin. *Biophys. J.* 77:2750–2763.

45. Béjà, O., L. Aravind, E. V. Koonin, M. T. Suzuki, A. Hadd, L. P. Nguyen, S. Jovanovich, C. M. Gates, R. A. Feldman, J. L. Spudich, E. N. Spudich, and E. F. DeLong. 2000. Bacterial rhodopsin: Evidence for a new type of phototrophy in the sea. *Science*. 289:1902–1906.

46. Wang, W.-W., O. A. Sineshchekov, E. N. Spudich, and J. L. Spudich. 2003. Spectroscopic and photochemical characterization of a deep ocean proteorhodopsin. *J. Biol. Chem.* 278:33985–33991.

47. Cha, K., F. J. Reeves, and H. G. Khorana. 2000. Structure and function in rhodopsin: Destabilization of rhodopsin by the binding of an antibody at the N-terminal segment provides support for involvement of the latter in an intradiscal tertiary structure. *Proc. Natl. Acad. Sci. USA*. 97:3016–3021.

48. Sudo, Y., M. Iwamoto, K. Shimono, and N. Kamo. 2002. Association between a photo-intermediate of a M-lacking mutant D75N of pharaonis phoborhodopsin and its cognate transducer. *J. Photochem. Photobiol. B*. 67:171–176.

49. Brown, L. S., A. K. Dioumaev, J. Lanyi, E. N. Spudich, and J. L. Spudich. 2001. Photochemical reaction cycle and proton transfers in *Neurospora* rhodopsin. *J. Biol. Chem.* 276:32495–32505.

50. TMHMM server version 2.0. http://www.cbs.dtu.dk/services/TMHMM/.